available at www.sciencedirect.com

ScienceDirect

www.elsevier.com/locate/brainres

BRAIN RESEARCH

Research Report

Paeonol increases levels of cortical cytochrome oxidase and vascular actin and improves behavior in a rat model of Alzheimer's disease

Jun Zhou[a], *Li Zhou*[a], *Deren Hou*[a], *Jiaochun Tang*[a], *Juanjuan Sun*[a], *Stephen C. Bondy*[b,*]

[a]*Center of Medical Research, Department of Radiology, and Neurology, Third Xiang-ya Hospital, Xiang-ya School of Medicine, Central Southern University 410013, Changsha, China*

[b]*Center for Occupational and Environmental Health, Department of Medicine University of California, Irvine, CA 92697-1825, USA*

ARTICLE INFO

Article history:
Accepted 21 February 2011
Available online 4 March 2011

Keywords:
Paeonol
Alzheimer's disease
β-Amyloid
Actin
Cytochrome oxidase

ABSTRACT

Paeonol(2′-hydroxy-4′-methoxyacetophenone;1-(2-hydroxy-4-methoxyphenyl)ethan-1-one) is a constituent of the bark of the Moutan Cortex (*Paeonia suffruticosa*). This bark has been used as a traditional Chinese medicine and is reputed to possess a broad range of therapeutic properties probably by virtue of its anti-inflammatory and free radical scavenging properties. The effects of paeonol on a variety of biochemical and behavioral parameters were studied in rat brain in rat brain after experimental animals had been subjected to an intra-hippocampal injection of amyloid peptide, Aβ1–42. Sprague–Dawley rats were randomly divided into groups: saline, sham operated, β-amyloid (Aβ)-injected (intended to model Alzheimer's disease, (AD), and a group receiving both injected amyloid peptide and paeonol. Forty days after intra-hippocampal injection, H&E staining revealed that the lesions in the paeonol-treated group were significantly less than the untreated group. Levels of cytochrome oxidase and α-actin, determined immunohistochemically, were elevated in the paeonol treated group relative to the group receiving amyloid peptide alone. TUNEL staining revealed more apoptotic cells in the walls of the cerebral vascular elements in the AD model group than in the paeonol group. The paeonol-treated group also showed improvement in behavioral indices of learning relative to the group receiving Aβ1–42 alone, as judged using a Y-type electric maze. Treatment with paeonol can protect against many of the alterations resulting from administration of Aβ1–42. in a rat model of AD. These include morphological, biochemical and behavioral changes. Paeonol is a possible therapeutic measure in slowing down the pathogenic processes associated with AD.

1. Introduction

Alzheimer's disease (AD) is a neurodegenerative disease resulting in progressive cognitive decline and is characterized by accumulation of ß-amyloid peptides (Aß) and neurofibrillary tangles (Yuan and Yankner, 2000). ß-amyloid peptide, a 39–42 residue proteolytic product of the amyloid protein precursor protein (APP), forms protease-resistant aggregates, which undergo further conformational change to form fibrillar β-sheets. It may cause neurotoxicity through various direct or indirect

* *Corresponding author*. Fax: 949 824 2793.
E-mail address: SCBONDY@UCI.EDU (S.C. Bondy).

0006-8993/$ – see front matter © 2011 Elsevier B.V. All rights reserved.
doi:10.1016/j.brainres.2011.02.064

mechanisms (Morris et al., 2001). The extent of deposition of Aß in dense senile plaques has been correlated with progression of cognitive dysfunction in AD (Ye and Qiao, 1999).

In AD patients, the antioxidant defense systems in the brain appear to be reduced, resulting in increased levels of oxidant species including superoxide anion radical, hydrogen peroxide, lipid peroxide (Ravindra et al., 2004). These species have the capacity to damage membrane components of organelles, and this can lead to elevated neuronal and cerebrovascular apoptosis (Miller et al., 2010). Mitochondria are a major site of production of free radicals (Shi and Gibson, 2007) and impaired mitochondrial function is characteristic of AD (Lin and Beal, 2006).

AD is a complex disease, and no single "magic bullet" is likely to prevent or cure it. However, AD research has developed to a point where scientists can look beyond treating symptoms to think about delaying or preventing AD by addressing the underlying disease process. Many possible interventions have been considered, including anti-inflammatory and antioxidant treatments, immunization therapy, cognitive training, changes in diet, and physical activity, in an effort to slow the disease, or help reduce symptoms. While the mechanism of this neurodegeneration remains to be defined, substantial evidence implicating a significant role for the Aß peptide has been reported (reviewed in Golde, 2005; Hardy and Selkoe, 2002).

Paeonol (2′-hydroxy-4′-methoxyacetophenone) is a major phenolic component of Moutan Cortex (*Paeonia suffruticosa*). It has been traditionally used as a Chinese herbal medicine in various diseases. It is known to possess anti-inflammatory and anti-proliferative activities. It is also sedative and analgesic and has been reported to protect against cerebrovascular damage (Xu et al., 2008).

The present investigation was designed to determine the effects of paeonol on Aß-induced brain damage in rats. In addition to study of some key enzymes involved in production of reactive oxygen species, apoptosis and a behavioral measure of learning ability were also examined.

Collectively, our results suggest that paeonol improved energy metabolism and alleviated the development of brain pathology as well as inhibiting neuron and vascular smooth muscle cell apoptosis. Due to its small molecular weight, and amphiphilic nature it appears able to penetrate the blood brain barrier and has been reported as neuroprotective (Hsieh et al., 2006). This study is based on the premise that paeonol may find utility as a therapeutic agent in the treatment of AD.

2. Results

2.1. *6E10 (A beta 1–16) immunostaining following paeonol administration*

Using the 6E10 antibody as definitive, β-amyloid proteins were not found in brain tissue from control (Fig. 1A) and sham-treated groups, but deposits were present in the AD model group, and Pae group in the cortex and hippocampus adjacent to the Aβ injection area. The extent of 6E10 antibody positive reaction within these two latter groups did not differ significantly (Fig. 1B and C)

2.2. *Effect of paeonol treatment on COX1 levels in hippocampal and cortical tissues*

Cytochrome oxidase 1 immunoreactivity was increased significantly over levels in the AD model group in neurons in Pae group (E, F) (Fig. 2C, D) and as shown by quantitative densitometric analysis (Fig. 2G) ($P<0.015$). However, these levels were not restored to those found in the control group. These findings suggest that the increase of COX1 in the peaonol group may be related to increased mitochondrial functioning.

2.3. *The effect of paeonol treatment on content of α-actin in smooth muscle cells within brainstem vasculature*

Levels of α-actin in vascular smooth muscle cells were decreased significantly in AD model group (Fig. 3C, D) relative to the control group (Fig. 3A, B). The concurrent application of paeonol to the Aβ group Fig. 3E, F) restored values so that they were statistically identical to those of the control group. These changes in actin content were confirmed by Western blot analysis (Fig. 3G).

The terminal deoxynucleotidyl transferase-mediated Digoxigenin-11-dUTP end labeling (TUNEL) method, labels fragmented DNA, which is a characteristic of the apoptotic cells. Few apoptotic cells were seen in the control group and these were never present in the vascular wall (Fig. 4A). TUNEL-positive cells were found in the brainstem in the Aβ model group (Fig. 4B) and Pae group (Fig. 4C). However, more apoptotic cells were apparent in the AD model group than in the Pae group ($P<0.05$). Thus, paeonol treatment attenuated Aβ-induced apoptosis in vascular smooth cell elements.

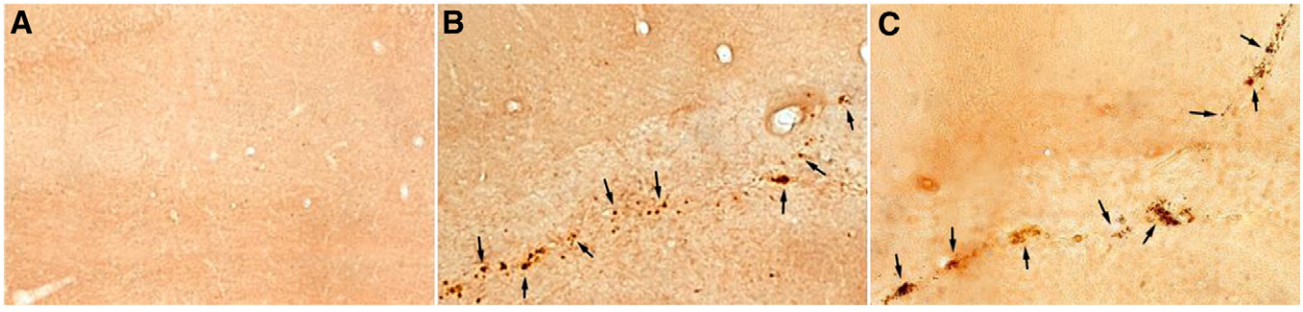

Fig. 1 – 6E10 staining in control group (A) AD model group (B) and Pae group (C), (×100) of hippocampus and cortex.

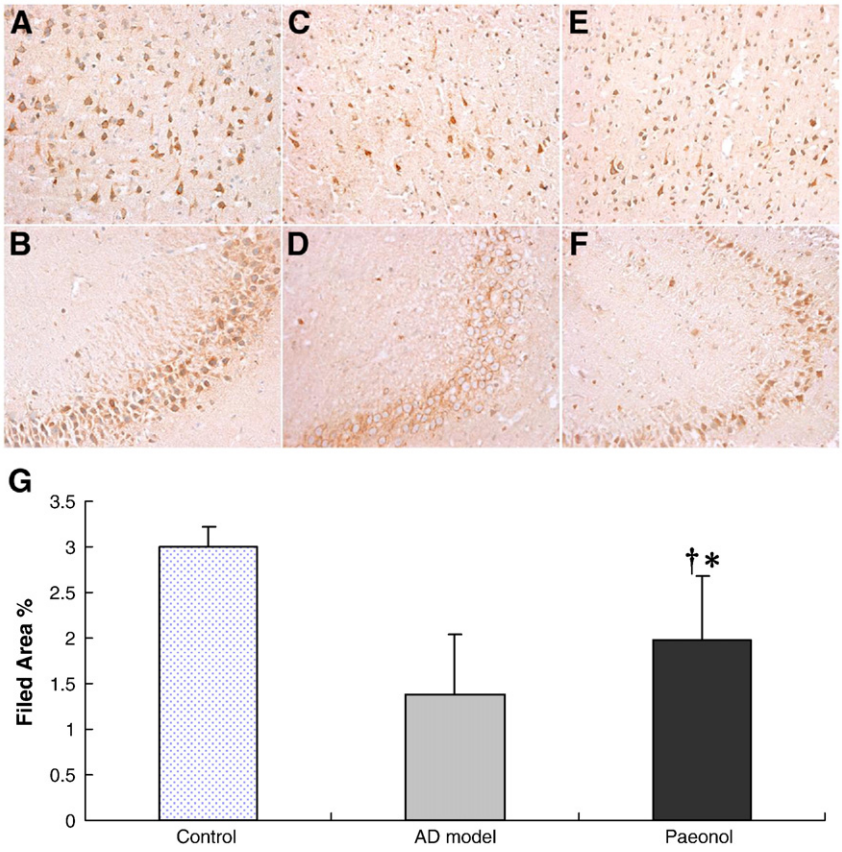

Fig. 2 – COX1 staining reaction. A, C, E are cortical sections and B, D and F are hippocampal sections around the CA3 region. A, B = control group, C, D = AD model group, E, F = Pae group. (×200) G = Quantitative densitometric analysis of hippocampus and cortex together. Values for the Pae group differed significantly from those of the control and AD model groups (*$P<0.015$).

2.4. *Differing behavioral characteristics of the experimental groups*

Rats were tested in a maze test box, and the rate of learning escape from administered electroshock was quantitated. Active escape capacity was diminished in the AD model group and this was partially reversed in the paeonol group (Fig. 5). This alleviation was significant in the paeonol group relative to the AD model group ($P<0.01$). There was no significant difference between the paeonol group and the control group ($P>0.05$).

3. Discussion

β-amyloid peptides are known to induce AD-like pathology *in vitro*, probably by way of enhancing apoptosis and decreasing mitochondrial function thereby impairing learning and memory (Zhang et al., 2008). Injection of Aβ peptides into the hippocampus of animals is a commonly used method to establish an AD animal model (Pike et al., 1997; Perry et al., 1998). Many studies have described parallels between the presence of endogenous Aβ1–42 and the administered peptide and the ability of either, to induce lesions and promote the pathological changes resembling those associated with AD (Zhang et al., 2006).

Effective prevention and control of Alzheimer's disease progression remains elusive. In this regard, the properties of some critical constituents of traditional Chinese medicine are emerging as an area of interest and investigation of their pharmacological properties is legitimate. The potential utility of paeonol in neuronal protection may reside in its antioxidant properties or its ability to inhibiting Ca^{2+} influx into the cell. Elevated intracellular Ca^{2+} can induce apoptosis (Huang et al., 1999).

The results from the immunohistochemistry of the 6E10 antibody suggest that our Aβ depositional model may find utility in that it led to the appearance of persistent and irresolvable macromolecular aggregates. The findings concerning COX 1 imply Aβ-induced damage to mitochondria. Mitochondrial dysfunction and neuroinflammatory processes may lead to an excess production of harmful reactive oxygen species (Witte et al., 2010). The finding Aβ treatment resulted in diminished levels of β-actin within the cerebral vasculature is in accord with a report that Aβ peptides are anti-angiogenic both *in vitro* and *in vivo* (Paris et al. 2004). It has been reported that the cerebral vasculature is compromised in the AD brain (Blass et al 2002).

There have been prior suggestions that paeonol may have a neuroprotective role. Behavioral deficits following administration of galactose, a neurotoxic agent, have been reversed (Zhong et al., 2009) and paeonol can prevent anoxic damage to

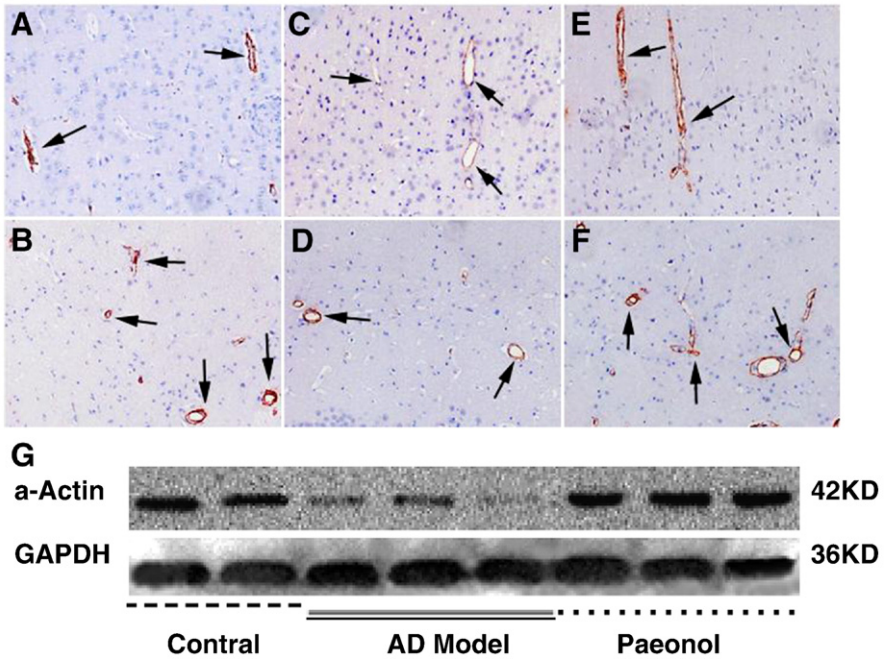

Fig. 3 – Content of α-actin in smooth muscle cells within cerebral vasculature. A, C, E are cortical sections and B, D and F are hippocampal sections around the CA3 region. A, B = control group, C, D = AD model group, E, F = Pae group (×100). Arrows indicate location of actin-staining elements. G = Western blot of α-actin levels in hippocampus and cortex of control (Cont), AD model (Mo) and paeonol (Pae) groups. Paeonol inhibited apoptosis of both neurons and vascular smooth cells.

nervous tissue (Hsieh et al., 2006; Wu et al., 2008). While in our study, paeonol appeared to mitigate Aβ-induced damage to the cerebral vasculature, paeonol has been reported as anti-angiogenic in a trial relating to its potential use in cancer treatment (Kim et al., 2009). Thus the effect on blood vessels is likely to be secondary to the anti-oxidant or anti-inflammatory properties of paeonol.

Paeonol intervention in AD model rats reduced the extent of the apoptosis and appeared to lessen Aβ-induced damage of the cerebral vasculature. Together with the partial alleviation of Aβ-induced behavioral deficits, these data suggest that paeonol may offer a protective strategy in the treatment of Alzheimer's disease.

In order to validate the utility of this compound, it is important to demonstrate a distinctive property that cannot readily be replicated by more conventional neuroprotectants. This requires better understanding of the underlying neuroprotective properties of paeonol. The primary mechanism of

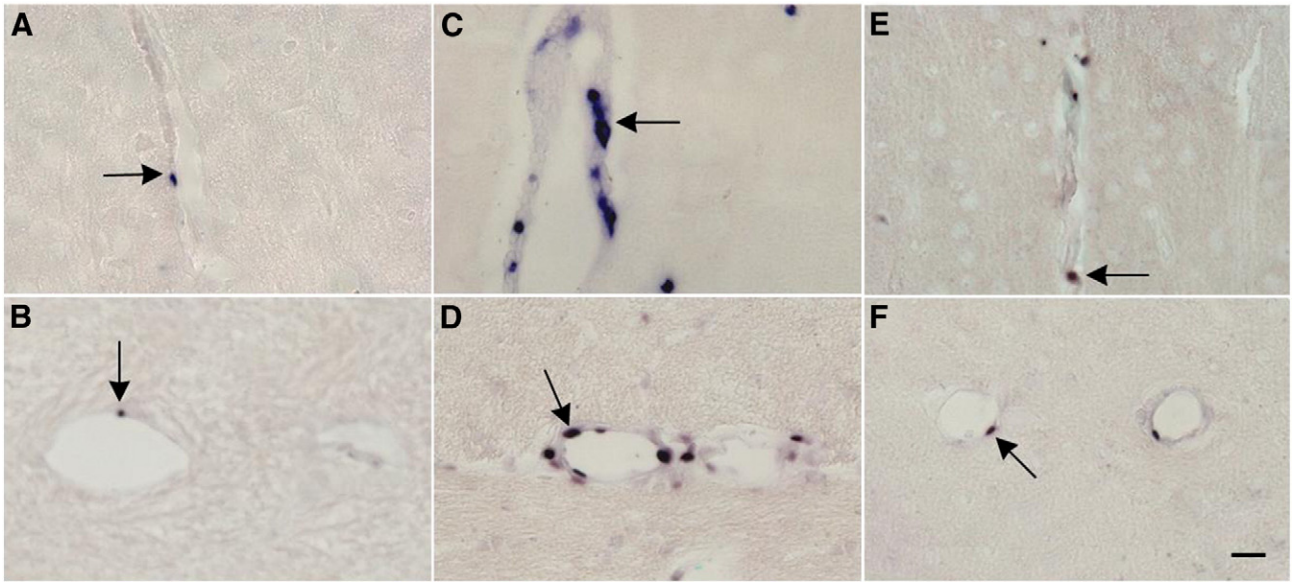

Fig. 4 – TUNEL staining in vascular smooth muscle cells and endothelial cells within the brainstem. A, B = control group; C, D = AD model group; E, F = Pae group (×400). Arrows indicate areas with apoptotic activity.

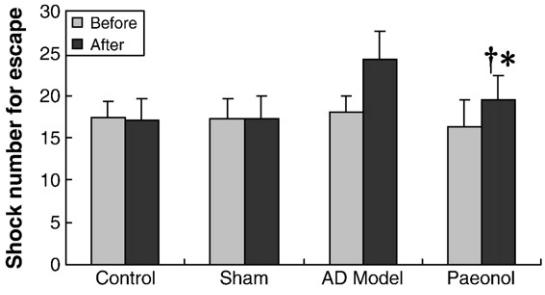

Fig. 5 – Rate of escape learning in experimental groups. Ordinate shows number of shocks applied before effective escape criteria are met. *Differs from corresponding value for control group, †differs from corresponding value for AD model group.

action of this however remains unclear. It has been reported as anti-inflammatory (Chae et al., 2009) perhaps by inhibition of TNFα release (Kim et al., 2004) with consequent reduction the NF-kB inflammatory cascade (Nizamutdinova et al., 2007). Alternatively, the initial site of action of paeonol has been posited to be inhibition of calcium fluxes (Li et al., 2010). Finally, paeonol undoubtedly has direct potent anti-oxidant activity. It is noteworthy that several of the glycoside esters of paeonol (suffruticosides) are reported to have greater antioxidant potency than that of α-tocopherol (Matsuda et al., 2001).

4. Experimental procedures

4.1. Materials

Paeonol (purity control>98%) was purchased from Natura-pharm, Inc. (Waare, Netherlands).

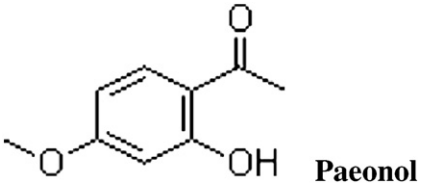

Paeonol

Aß1–42 peptide was from Sigma (St. Louis, MO, USA). Amyloid peptide fibril was prepared by resuspension of 1 mg lyophilized Aß1–42 peptide in 500 μl physiological saline followed by incubation at 37 °C with continuous stirring for a week. Then Aß1–42 peptide was then in a state of aggregation and was stored at 4 °C before being used.

4.2. Animals and grouping

A total of 32 Sprague–Dawley male rats, weighing 220–240 g, were used. The rats were obtained from the Animal Center of Central South University and were housed in standard cages in the animal center of the Central South University. Humidity levels were maintained at 55±5%, and the rats were kept in a 12-h light–dark cycle at 22±2 °C. All animal experiments were performed in accordance with the Guidelines of the Chinese Society for Laboratory Animal Science. The rats were divided into 4 groups of eight rats as follows: (1) *control* group rats received phosphate-buffered saline (1.0 ml/kg i.p., daily); (2) *sham* operated group animals received the same daily i.p. injections of saline and surgical procedures as the DA model group but without Aß1–42 peptide injection; (3) the *AD model* group received a single intrahippocampal injection of 10 μl Aß1–42 peptide at the beginning of the study in addition to daily i.p. injection of saline; (4) the *paeonol* group was treated as the AD model group but also received paeonol (5 mg/kg, i.p.) immediately after Aß1–42 peptides injection, and then every 24 h for a further 40 days). After 40 days, all rats were behaviorally tested and then killed and the brains removed for histology and immunohistochemistry and Western blotting.

4.3. Surgical procedures

Rats were anesthetized with 10% chloral hydrate (350 mg/kg, i.p.) and then were placed in a stereotactic apparatus in the prone position. The skin was incised along the midline to reveal the frontal fontanelle. The target coordinates for the right hippocampus were 3.0 mm posterior of the frontal fontanelle, 2.0 mm right of the midline, and 2.8 mm ventral of the surface of the cortex. Using a 20-μl Hamilton Syringe, Aß1–42 peptides were injected into this coordinate. The Aß1–42 was injected at a rate of 1.0 μl/10 min with a 1-min pause between each 5 μl and a 5-min delay before syringe withdrawal. The incision was carefully sutured. Body temperature was maintained during recovery at 37 °C by means of a servocontrolled system consisting of a rectal temperature probe and a heating lamp. Sham animals received the same surgical procedures including drilling of the burr holes and were anesthetized for the same duration as the rats of the AD model and paeonol groups.

4.4. Behavioral analysis of rats

Rats were subjected to a learning and memory capacity test involving a Y-type electric maze. They were placed inside the maze for 4 min. Taking one limb of the Y resulted in rats being shocked with an electrical current (50 V, 0.6 mA). The animals were monitored and the rate of learning to escape to the safe arm of the maze was determined for each animal. Upon electrical stimulation, direct escape from the primary region to the safe region was considered to be the correct reaction.

The Y-type electric maze (or Trisection radiant maze) was used to test learning and memory of the rats. The rats were placed beside the Y-type electric maze, allowed to adapt to the environment for 5 min, and then testing began randomly starting from one direction. Electrical current (30–70 V, 0.5–0.7 mA) was used for shock administration. The time needed for escape electrical stimulation to the safe region was utilized in order to quantitate learning and memory abilities in the rats. Between every two tests, there was a 30-second rest, with 5 min between every 10 tests. The animals were considered to have learned the maze with 9/10 correct choices during continuous testing. A smaller value was assumed to reflect

improved learning. Rats that did not correctly choose escape during testing with electrical stimulation shock had a lower score.

4.5. Brain sample preparation

Rats were deeply anesthetized with an overdose of 10% chloral hydrate and then perfused transcardially with cold 0.1 M phosphate-buffered saline pH 7.4 (PBS). After dissection one half of the brain was immediately frozen on dry ice (for Western blots) and the other half fixed overnight with paraformaldehyde (4% in 0.1 M PBS for immunohistochemistry and TUNEL staining). Thereafter, fixed tissue was stored in PBS/0.02% Na azide at 4 °C until use. Finally, the fixed brain tissue was further processed by dehydration in a series of graded ethanol solutions prior to paraffin embedding. The blocks were cut in serial 5-μm-thick sections and mounted on adhered slides pretreated with vectabond reagent (Vector Laboratories, Burlingame, CA, USA) in a water bath at 45 °C. Tissue slides were stored at 4 °C before being stained.

4.6. Immunohistochemistry

Deparaffinization was performed by heating the sections for 25 min at 56 °C. The tissue was then dehydrated twice using a xylene bath and a graded series of ethanol. Immunohistochemistry was performed on paraffin embedded sections. Sections were immersed in antigen unmasking solution (Vector Laboratories, Burlingame, CA, USA) for 20 min with 80 °C. Endogenous peroxidase in tissue was blocked by treating with 3% H_2O_2 in PBS, 20 min at room temperature. Nonspecific background staining was blocked by a 1-h incubation in 2% BSA with 0.3% Triton X-100. Sections were then incubated with primary antibodies (6E10 1:1000 Signet; COX1 1:100, Santa Cruz Biotechnology, Santa Cruz, CA, USA), α-actin 1:1000 (R&D Systems, Inc., Minneapolis, MN, USA) overnight at 4 °C, then rinsed in PBS with 0.1%TX and incubated with biotinylated secondary antibody (Vector) and streptavidin–horseradish peroxidase (Jackson ImmunoResearch, West Grove, PA, USA) for 1 h each at room temperature. Finally, the sections were incubated for approximately 2–5 min with diamino-benzidine (DAB) (Vector) for color developing. Sections were further processed by dehydration in a series of graded ethanol, cleared with xylene, and then coverslipped with DPX (Biomedical Specialties, CA). As controls, sections were incubated in parallel without primary antibody and these sections failed to develop specific staining.

4.7. Western blotting

Samples of cortex and hippocampus together were prepared from fresh frozen brain tissue and homogenized in 10 volumes extraction ice-cold tris-buffered saline (20 mM Tris–HCl buffer pH 7.4, 150 mM NaCl) (0.150 g tissue/2 ml buffer) with 0.5 mM phenylmethylsulfonyl fluoride and a Protease Inhibitor cocktail from Sigma. Homogenates were centrifuged at 15,000×*g* for 30 min. Protein concentration in the supernatants was determined with BCA protein assay (Novagen Inc. Madison, WI). Samples (50 μg protein per lane) were run on 10% SDS polyacrylamide gel under reducing conditions. Proteins were transferred to polyvinylidene difluoride (Amersham Biosciences, Piscataway, NJ) membrane (300 mA for 1.5 h). Membrane was blocked with 3% dry milk in 0.1% Tween/TBS for 1 h, then incubated for 2 h at RT with a-Actin antibody(R&D systems, Inc., Minneapolis, MN) at 1 μg/ml. After washing, blots were incubated with the corresponding HRP-labeled secondary antibodies (1:10 k dilution from Jackson Labs, Bar Harbor, ME) for 1 h. Labeling was detected using an enhanced chemiluminescence (ECL) system (Thermo Scientific, Rockford, IL). Blots were stripped following manufacturer's instructions (Thermo Scientific) and subsequently labeled with GAPDH antibody(1:300 Chemicon Int., Temecula, CA) following same procedures as above.

4.8. TUNEL staining

After deparaffinization, the sections were rinsed with 0.1 M PBS, pH 7.4, for 10 min at room temperature (RT), treated with 0.3% Triton X-100 in 0.1 M PBS for 15 min at RT, and rinsed in 0.1 M PBS. The sections were treated with proteinase K (Sigma) 2 μg/ml in 0.1 M PBS for 15 min at RT. The sections were washed in 0.1 M for 5 min at RT, and then incubated in 0.25% acetic anhydride (Sigma) in water for 30 min at RT. After a wash in sterile dH_2O for 5 min, the sections were incubated with prehybridization solution (0.14 M Na cacodylate, 1 mM cobalt chloride, 0.03 Tris–HCl, pH 7.2) for 10 min at RT. The prehybridization solution was then replaced with hybridization solution (prehybridization solution with reaction mixture: 40 U/ml deoxynucleotidyl transferase enzyme, 0.2 mg/ml BSA and 0.5 nM/ml digoxigenin-11-dUTP) for 2 h at 37 °C. Sections were washed twice for 20 min in 2× SSC, then washed two more times in 1× SSC for 15 min and 0.5× SSC for 15 min at room temperature.

Next, sections were washed in 0.1 M Tris for 15 min, pH 7.5, incubated in anti-DIG-11 (Roche, Nutley, NJ) at 1:1000 in Tris buffer with 2% BSA for 1 h and 30 min, then washed 3 times for 15 min in Tris at RT. The sections were next immersed in Tris buffer with 0.1 M NaCl and 0.05 M MgCl2, pH 9.5, for 15 min, and incubated in Tris buffer in the presence of nitroblue tetrazolium and 5-bromo-4-chloro-3-indolyl phosphate (Roche) for color development. Sections were rinsed several times in 0.01 M Tris buffer with 1 mM EDTA and then mounted on glass slides with water-soluble mounting medium.

4.9. Image and statistical analysis

Immunostaining was observed under a Nikon Eclipse 80i microscope (Nikon, Japan) and images acquired with a Nikon DS high-resolution digital color camera (1280×1024 pixel) using NIS-Elements AR 3.0 software. Digital images were analyzed using Ver.3.00 analysis program (Nikon). Percentage of immunostained area (field area of immunostaining/total image area×100) was determined for all the markers studied by averaging several images per section that cover all or most of the region of study. All experiments were repeated at least twice, with $n=6–8$ animals per group per marker. All quantitative comparisons were performed on sections processed at the same time. Single ANOVA statistical analysis was used to assess the significance of the differences in anti-COX1, anti α-actin and TUNEL staining reactivity among the animal groups.

REFERENCES

Blass, J.P., Gibson, G.E., Hoyer, S., 2002. The role of the metabolic lesion in Alzheimer's disease. J. Alz. Dis. 4, 225–232.

Chae, H.S., Kang, O.H., Lee, Y.S., Choi, J.G., Oh, Y.C., Jang, H.J., Kim, M.S., Kim, J.H., Jeong, S.I., Kwon, D.Y., 2009. Inhibition of LPS-induced iNOS, COX-2 and inflammatory mediator expression by paeonol through the MAPKs inactivation in RAW 264.7 cells. Am. J. Chin. Med. 37, 181–194.

Golde, T.E., 2005. The Abeta hypothesis: leading us to rationally-designed therapeutic strategies for the treatment or prevention of Alzheimer disease. Brain Pathol. 15, 84–87.

Hardy, J., Selkoe, D.J., 2002. The amyloid hypothesis of Alzheimer's disease: progress and problems on the road to therapeutics. Science 297, 353–356.

Hsieh, C.L., Cheng, C.Y., Tsai, T.H., Lin, I.H., Liu, C.H., Chiang, S.Y., Lin, J.G., Lao, C.J., Tang, N.Y., 2006. Paeonol reduced cerebral infarction involving the superoxide anion and microglia activation in ischemia–reperfusion injured rats. J. Ethnopharmacol. 106, 208–215.

Huang, X., Atwood, C.S., Hartshorn, M.A., Multhaup, G., Goldstein, L.E., Scarpa, R.C., Cuajungco, M.P., Gray, D.N., Lim, J., Moir, R.D., Tanzi, R.E., Bush, A.I., 1999. The Aβ peptide of Alzheimer's disease directly produces hydrogen peroxide through metal ion reduction. Biochemistry 38, 7609–7616.

Kim, S.A., Lee, H.J., Ahn, K.S., Lee, H.J., Lee, E.O., Ahn, K.S., Choi, S.H., Jung, S.J., Kim, J.Y., Baek, N., Kim, S.H., 2009. Paeonol exerts anti-angiogenic and anti-metastatic activities through downmodulation of Akt activation and inactivation of matrix metalloproteinases. Biol. Pharm. Bull. 32, 1142–1147.

Kim, S.H., Kim, S.A., Park, M.K., Kim, S.H., Park, Y.D., Na, H.J., Kim, H.M., Shin, M.K., Ahn, K.S., 2004. Paeonol inhibits anaphylactic reaction by regulating histamine and TNF-alpha. Int. Immunopharmacol. 4, 279–287.

Li, Y.J., Bao, J.X., Xu, J.W., Murad, F., Bian, K., 2010. Vascular dilation by paeonol—a mechanism study. Vasc. Pharmacol. 53, 169–176.

Lin, M.T., Beal, M.F., 2006. Mitochondrial dysfunction and oxidative stress in neurodegenerative diseases. Nature 443, 787–795.

Matsuda, H., Ohta, T., Kawaguchi, A., Yoshikawa, M., 2001. Bioactive constituents of Chinese natural medicines. VI. Moutan cortex. (2): structures and radical scavenging effects of suffruticosides A, B, C, D, and E and galloyl-oxypaeoniflorin. Chem. Pharm. Bull. (Tokyo) 49, 69–72.

Miller, A.A., Budzyn, K., Sobey, C.G., 2010. Vascular dysfunction in cerebrovascular disease: mechanisms and therapeutic intervention. Clin. Sci. (Lond.) 119, 1–17.

Morris, J.C., Storandt, M., Miller, J.P., McKeel, D.W., Price, J.L., Rubin, E.H., Berg, L., 2001. Mild cognitive impairment represents early-stage Alzheimer disease. Arch. Neurol. 5, 397–405.

Nizamutdinova, I.T., Oh, H.M., Min, Y.N., Park, S.H., Lee, M.J., Kim, J. S., Yean, M.H., Kang, S.S., Kim, Y.S., Chang, K.C., Kim, H.J., 2007. Paeonol suppresses intercellular adhesion molecule-1 expression in tumor necrosis factor-alpha-stimulated human umbilical vein endothelial cells by blocking p38, ERK and nuclear factor-kappaB signaling pathways. Int. Immunopharmacol. 7, 343–350.

Paris, D., Townsend, K., Quadros, A., Humphrey, J., Sun, J., Brem, S., Wotoczek-Obadia, M., DelleDonne, A., Patel, N., Obregon, D.F., Crescentini, R., Abdullah, L., Coppola, D., Rojiani, A.M., Crawford, F., Sebti, S.M., Mullan, M., 2004. Inhibition of angiogenesis by Abeta peptides. Angiogenesis 7, 75–85.

Perry, G., Castellani, R.J., Hirai, K., Smith, M.A., 1998. Reactive oxygen species mediate cellular damage in Alzheimer disease. J. Alz. Dis. 1, 45–55.

Pike, C.J., Ramezan Arab, N., Cotman, C.W., 1997. β Amyloid neurotoxicity in: vitro evidence of oxidative stress but not protection by antioxidants. J. Neurochem. 69, 1601–1609.

Ravindra, P.S., Pratap, S., Shashwat, S., Suman, K., 2004. Free radicals and oxidative stress in neurodegenerative diseases: relevance of dietary antioxidants. J. Ind. Acad. Clin. Med. 5, 218–225.

Shi, Q., Gibson, G.E., 2007. Oxidative stress and transcriptional regulation in Alzheimer disease. Alz. Dis. Assoc. Disord. 21, 276–291.

Witte, M.E., Geurts, J.J., de Vries, H.E., van der Valk, P., van Horssen, J., 2010. Mitochondrial dysfunction: a potential link between neuroinflammation and neurodegeneration? Mitochondrion 10, 411–418.

Wu, J.B., Song, N.N., Wei, X.B., Guan, H.S., Zhang, X.M., 2008. Protective effects of paeonol on cultured rat hippocampal neurons against oxygen–glucose deprivation-induced injury. J. Neurol. Sci. 264, 50–55.

Xu, D., Zhou, C., Xu, B., 2008. Protective effect of paeonol on beta-amyloid 25–35 induced toxicity in PC12 cells. Neural Regen. Res. 3, 863–866.

Ye, L., Qiao, J.T., 1999. Suppressive action produced by beta-amyloid peptide fragment 31–35 on long-term potentiation in rat hippocampus is *N*-methyl-D-aspartate receptor-independent: it's offset by huperzine. Neurosci. Lett. 275, 187–190.

Yuan, J., Yankner, B.A., 2000. Apoptosis in the nervous system. Nature 407, 802–809.

Zhang, H.Y., Zheng, C.Y., Yan, H., Wang, Z.F., Tang, L.L., Gao, X., Tang, X.C., 2008. Potential therapeutic targets of huperzine A for Alzheimer's disease and vascular dementia. Chem. Biol. Interact. 175, 396–402.

Zhang, J.M., Wu, M.N., Qi, J.S., Qiao, J.T., 2006. Amyloid beta-protein fragment 31–35 suppresses long-term potentiation in hippocampal CA1 region of rats in vivo. Synapse 60, 307–313.

Zhong, S.Z., Ge, Q.H., Qu, R., Li, Q., Ma, S.P., 2009. Paeonol attenuates neurotoxicity and ameliorates cognitive impairment induced by d-galactose in ICR mice. J. Neurol. Sci. 277, 58–64.